Electronic Supplementary Material (ESI) for Journal of Materials Chemistry C.

SUPPORTING INFORMATION

Impact of molecular conformation on triplet-fusion induced photon energy up-conversion in the absence of exothermic triplet energy transfer

Hossein Goudarzi [a], Saurav Limbu [b], Juan Cabanillas-González [c], Vassiliki M. Zenonos [d], Ji-Seon Kim [b], Panagiotis E. Keivanidis [d]*

[a] Centre for Nano Science and Technology @PoliMi, Fondazione Istituto Italiano di Tecnologia, Via Pascoli 70/3, 20133 Milano, Italy

[b] Imperial College London, Blackett Laboratory, Prince Consort Road, London SW7 2AZ, UK

[c] Fundacion IMDEA Nanociencia, Calle Faraday 9, Ciudad Universitaria de Cantoblanco, Madrid, ES 28049

[d] Department of Mechanical Engineering and Materials Science and Engineering, Cyprus University of Technology, Limassol 3041, Cyprus

Experimental Section

Thin films of PFO:PtOEP blends were fabricated by spin-coating of solutions based on the organic solvents of chloroform and toluene. Both solvents were thoroughly degassed, and the processes of solution preparation and thin film deposition were performed in a nitrogen-filled glove box. For reference purposes PF26:PtOEP, PS:PtOEP, PFO-only and PF26-only films were also developed and studied in an identical fashion. All polymer:PtOEP solutions were prepared with a concentration of 10 mg/ml in respect to polymer mass, while the PtOEP content was kept to 6 wt%. Spin-coating of these solutions was performed at 1200 rpm for 180 sec. All materials used in this study were used as received by commercial suppliers. Both poly(fluorene) (PF) derivatives were purchased from American Dye Source, Inc., PS was purchased from Sigma-Aldrich, Inc. and PtOEP was purchased from Frontier Scientific, Inc. Prior to film deposition, the quartz substrates were cleaned with surfactant (Helamanex III) and bi-distilled water. UV-Vis absorption spectra of all films were recorded with a use of a Shimadzu UV-2700 UV-Vis spectrometer. Time-integrated and time-gated PL spectra of the studied systems were recorded in a range of temperatures between 100 K and 290 K and for different pulsed laser photoexcitation intensities at 532 nm with the set-up described in Ref. [16, 17] of the main text. All data presented in this work were received for a photoexcitation pulse energy of 290 μJ except when a photoexcitation intensity dependent study was performed. In order to avoid degradation of the films induced by local laser heating effects, no focal lens was used for photoexcitation and the size of the spot size was kept to 0.385 cm^2. For registering the time-integrated TTA-UC spectra in the spectral region of 400 – 500 nm, a band pass filter (315 - 445 nm and 715 - 1095 nm) was used. Raman spectra of the PFO:PtOEP 6 wt% films spun from chloroform and toluene were recorded via Renishaw inVia Microscope in a backscattering configuration with Argon-ion Laser source for 457 nm excitation. The samples

were measured in a Linkam THMS600 stage under N_2 environment with ~20 μm defocused laser beam to avoid any laser-induced degradations to the films. Continuous-wave (cw) photoinduced absorption (PIA) experiments were performed exciting the samples with two different diode pumped solid state lasers (λ= 405 and λ= 532 nm) operating in cw regime. The excitation lines were mechanically chopped at 80 Hz and subsequently focused on the sample, (power densities at 405 and 532 nm were 15 and 46 $mWcm^{-2}$ respectively). The light from a Tungsten Halogen lamp (Spectral Products) was filtered by a 1/8 m monochromator (CM110 Spectral Products) equipped with a grating of 600 lines mm^{-1} and 500 nm efficiency peak and 600 μm slits. After passing through the monochromator, the light was focused on the sample and spatially superposed with the excitation spot. Phase sensitive detection of the transmitted light was performed with a dual lock-in amplifier (SR830 DSP Stanford Research) referred to the chopping frequency in combination with a liquid N_2-cooled InSb photodetector (Teledyne - Judson Technologies). The experiment was controlled by a home-made software which scanned the monochromator in 2 nm steps and recorded the lock-in amplifier readings at each wavelength. Prior to each measurement, a portion of laser scattering was deliberately sent to the photodetector by means of a flip mirror to set the zero-phase angle. The samples were enclosed on a continuous flow cryostat (Optistat CFV, Oxford Instruments) and all the experiments were performed at 77 K.

Raman Spectroscopy

The Raman data presented in Figure 2d of the main manuscript are in excellent agreement with previous literature related to Raman studies of the PFO derivative [Arif M. et al, Phys. Rev. Lett. 2006, 96, 025503; Volz C. *et al*, The Journal of Chemical Physics 2007, 126, 064905; Tsoi W. C. *et al*, Journal of Physics: Condensed Matter 2008, 20, 125213]. Table S1 below presents the assignment of the main Raman peaks to the vibrational modes of the PFO component in the PFO:PtOEP blend films.

Mode	**Center of Raman Peak (cm^{-1})**	**Relative peak intensity in PFO:PtOEP 6 wt% from toulene**	**Relative peak intensity in PFO:PtOEP 6 wt% from $CHCl_3$**
In-plane C-H bending and phenyl ring distortion	1135	0.11	0.06
Inter-ring C-C stretching	1219	0.04	0.02
Inter-ring C-C stretching	1233	0.04	0.02
Inter-ring C-C stretching and In-plane C-H bending	1256	0.08	0.03
C-C stretch between monomers	1282	0.11	0.07
C-C stretch between monomers	1307	0.07	0.06
C-C rocking between monomers	1346	0.08	0.07 (at 1352 cm^{-1})

Table S1. The main vibrational modes of the PFO component in the PFO:PtOEP blend films in correlation with the corresponding Raman peaks in the Raman spectra presented in Figure 2d of the main manuscript.

Time-integrated PL spectroscopy

Numerous detailed studies have already established rigorous correlations between processing conditions/structure/photophysical properties for the poly(fluorene-di-octyl) derivative in the solid state [*i.e.* Khan, A. L. T. *et al*, Synth. Met. 2003, 139, 905-907; Rothe, C. *et al*, Phys. Rev. B 2004, 70, 195213; Winokur, M. J. *et al*, Phys. Rev. B 2003, 67 (18), 184106; Hamilton I. *et al*, ACS Appl. Mater. Interfaces 2018, 10, 11070-11082]. Accordingly, we have acquired additional UV-Vis and PL spectra for a set of PFO-only films cast from $CHCl_3$ and toluene, presented in Figure S1 below. The overview of the registered PFO-only spectra corroborates the findings presented in the main manuscript in Figures 2b,c (UV-Vis spectra) and Figure 3 (PL spectra). As such the spectral narrowing and red-shifting that is observed in the toluene-cast PFO:PtOEP blend (see Figure 3 in our manuscript) are in agreement with all previous literature dedicated on the effect of β-phase formation in PFO films.

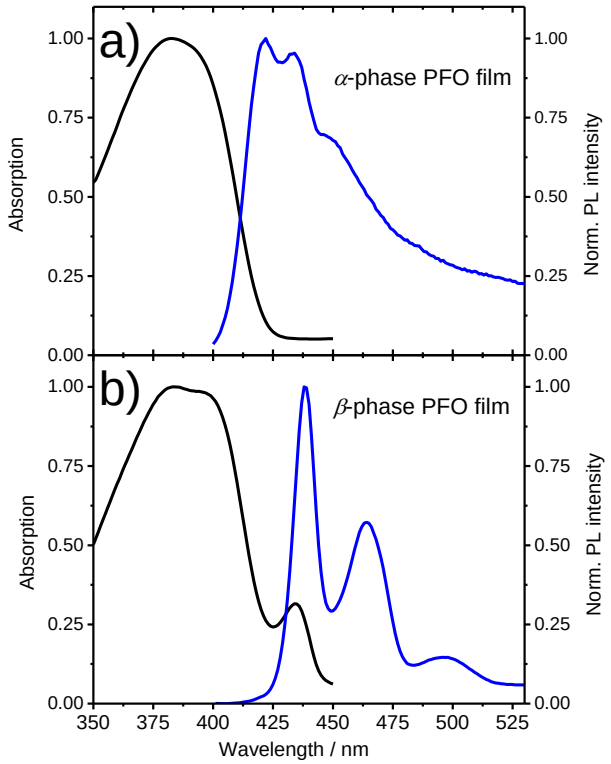

Figure S1. Normalized UV-Vis absorption spectra (black lines) and time-integrated PL spectra (blue lines) for PFO-only films spin-coated from solutions of a) $CHCl_3$ and b) toluene. In both cases, photoexcitation of the films was at 380 nm.

Based on the optical absorption spectrum of PFO (see Figure S1 above), the main π-π* absorption peak of the *α*-phase is located at 383 nm, corresponding to an energy of $E_{S1\text{-}PFO\ \alpha\_phase}$ = 3.23 eV. The spectral signature of the *β*-phase absorption is detected at 435 nm, corresponding to an energy of $E_{S1\text{-}PFO\ \beta\_phase}$ = 2.83 eV. The PL spectrum of PFO peaks at 420 nm, corresponding to an energy of $E_{S1\text{-}PFO\ \alpha\_phase}$= 2.95 eV whilst for the *β*-phase PFO the PL peaks at 435 nm, corresponding to an energy of $E_{S1\text{-}PFO\ \beta\_phase}$= 2.83 eV. From previous studies it is known that the triplet energy levels of the α-phase and the *β*-phase PFO are placed at $E_{T1\text{-}PFO\ \alpha\_phase}$= 2.15 eV and $E_{T1\text{-}PFO\ \beta\_phase}$= 2.08 eV [Rothe C. *et al*, Phys. Rev. B 2004, 70, 195213].

Likewise, Figure S2 below present the UV-Vis absorption and PL spectra of a poly(styrene) (PS):PtOEP 6 wt% film. From the optical absorption spectra of PtOEP, the electronic transitions

that correspond to the S_1 (Q-band, 536 nm) and S_2 (Soret-band, 383 nm) electronic states are placed to $E_{S1\text{-}PtOEP}$= 2.31 eV and to $E_{S2\text{-}PtOEP}$= 3.23 eV, respectively. The energy of the T_1 triplet level for PtOEP can be determined by the peak of the PtOEP phosphorescence spectrum at 644 nm; that is an energy of $E_{T1\text{-}PtOEP}$= 1.92 eV. The annihilation of two triplet PtOEP excitons results in the summing of two triplet PtOEP quanta and in the activation of a higher lying state D^*_{PtOEP} with energy of $E_{D^*\text{-}PtOEP} = 2 \times E_{T1\text{-}PtOEP} = 2 \times 1.92$ eV= 3.84 eV.

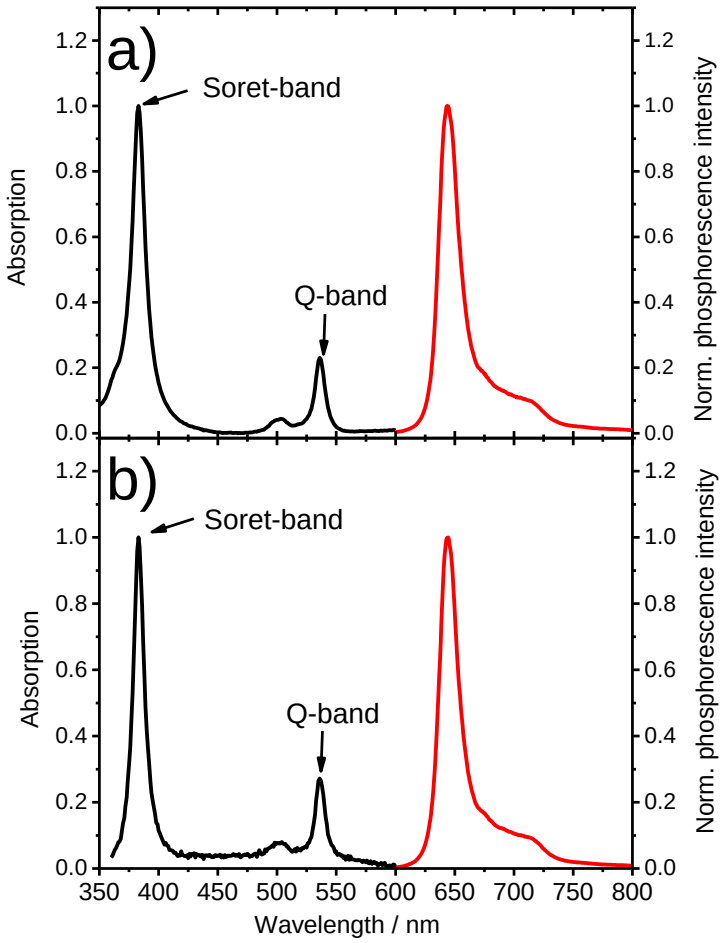

Figure S2. Normalized UV-Vis absorption spectra (black lines) and time-integrated phosphorescence spectra (red lines) for PS:PtOEP 6 wt% films spin-coated from solutions of a) $CHCl_3$ and b) toluene. In both cases, photoexcitation of the films was at 532 nm.

Figure S3 presents the time-integrated PL spectra of a PF8-only film obtained by excitation at 380 nm, and of a PFO:PtOEP blend film obtained by excitation at 532 nm. For the latter a band pass filter transmitting at 315 - 445 nm and 715 - 1095 nm is used, and the percentage transmittance (%T) of the filter is also shown for clarity. The lower transmittance of the filter in the spectral region at 460 nm underestimates the PL intensity of the the 0-1 peak in respect to the 0-0 peak.

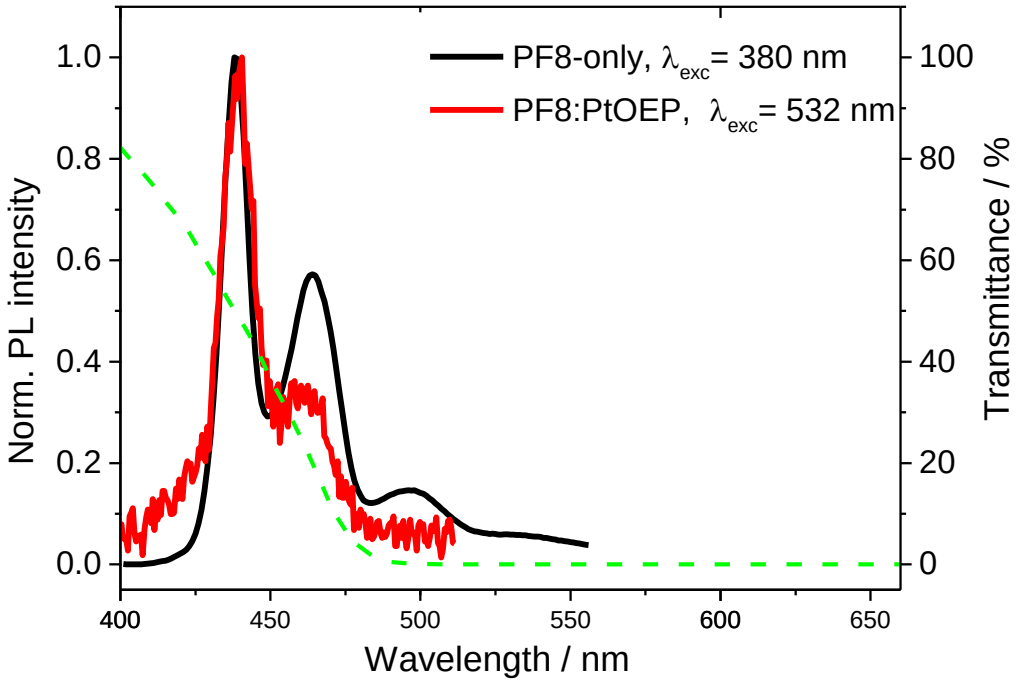

Figure S3. Normalized time-integrated PL spectra of a PF8-only film (black line) obtained by excitation at 380 nm, and a PFO:PtOEP blend film (red line) obtained by excitation at 532 nm. Both films are developed by toluene. For registering the up-converted PL spectrum of the PFO:PtOEP blend film a band pass filter was used transmitting at 315 - 445 nm and 715 - 1095 nm. The %T spectral window of the band pass filter is also shown as a green-dash line.

Time-gated PL spectroscopy

Time-gated TTA-UC PL kinetics

The TTA-UC luminescence kinetics of the PFO:PtOEP and PF26:PtOEP films spun from both solvents of chloroform ($CHCl_3$) and toluene are presented in Figure S4 below, both is the raw-data (Figure S4a, S4b) and normalized-data (Figure S4c, S4d) format.

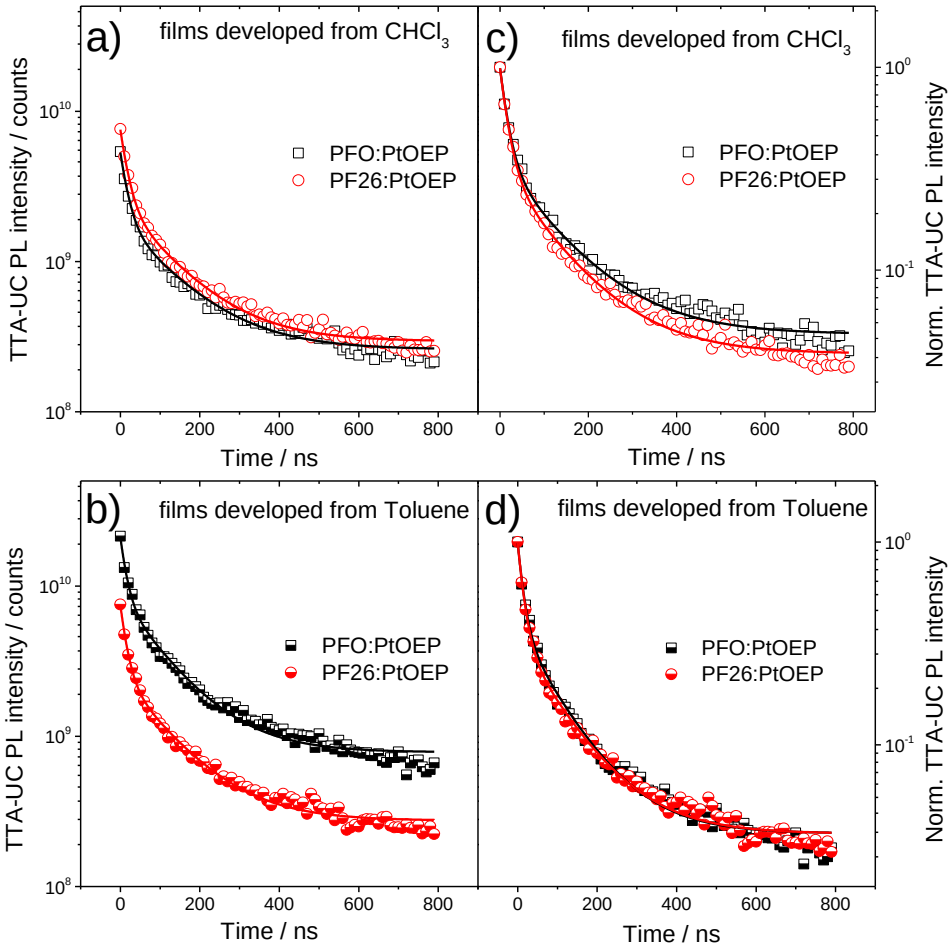

Figure S4. a) TTA-UC luminescence transients of PFO:PtOEP (open squares) and PF26:PtOEP (open circles) blend films spun from $CHCl_3$. b) TTA-UC luminescence transients of PFO:PtOEP (semi-filled squares) and PF26:PtOEP (semi-filled circles) blend films spun from toluene. c) Normalized TTA-UC luminescence transients of (a). d) Normalized TTA-UC luminescence transients of (d). In all cases the solid lines correspond to bi-exponential fits on the data (see Table R1). The data in a) and b) are corrected for the absorptance (1-T) of the films at the excitation wavelength 532 nm.

The obtained TTA-UC PL transients are best described by a bi-exponential function, and the average TTA-UC luminescence lifetime is in the order of 100 ns; that is much shorter than the lifetime of the PtOEP phosphorescence and the typical poly(fluorene) phosphorescence that are both in the time scale of μs. Yet, the observed TTA-UC luminescence lifetimes are much longer lived than the fluorescence lifetime of poly(fluorene) derivatives that typically corresponds to a fraction of a ns [Ariu M. *et al*, Phys. Rev. B: Condens. Matter Mater. Phys. 2003, 67, 195333; Becker, K., Adv. Funct. Mater. 2006, 16, 364−370], confirming the link of this TTA-UC emissive process with a meta-stable excited state. Table S2 below reports the amplitude and the respective lifetime values of each component as obtained by the bi-exponential fit of the normalized transient PL data. Notably, the *β*-phase of PFO-based sample spun from toluene exhibits a small reduction in the TTA-UC lifetime in comparison with the system spun from chloroform. This is attributed to the longer effective conjugated length [Grell, M. *et al*, Adv. Mater. 1997, 9, 798-802] of the *β*-phase PFO conformation that extends the PFO transition dipole moment and increases the corresponding radiative rate. Even so, the TTA-UC PL transient of this sample (Fig. S4a) verifies that the obtained time-gated TTA-UC PL intensity is much higher than in all the rest samples studied.

The obtained TTA-UC luminescence transients of the *β*-phase containing PFO:PtOEP blends verify that the TTA-UC emission intensity is unexpectedly stronger in respect to rest of the samples investigated. The monitored emission relates to an excited state with a metastable character, as it should be expected for a type of delayed luminescence. Moreover, this emissive transition is shorter-lived than the PtOEP triplet excite state confirming that is limited by an antagonistic fast deactivation channel. This agrees with the proposed PtOEP doubly photoexcited state which participates in the generation of TTA-UC luminescence in these systems; following the TTA-

mediated activation of the PtOEP doubly photoexcited state D^*_{PtOEP}, energy transfer to poly(fluorene) competes strongly with internal conversion in the first PtOEP singlet state (see state diagram shown in Figure 7 of the manuscript).

System	$A_1 \pm dA_1$	$\tau_1 \pm d\tau_1$ (ns)	$A_2 \pm dA_2$	$\tau_2 \pm d\tau_2$ (ns)	$y_0 \pm dy_0$	$<\tau>$ (ns)
PFO:PtOEP – $CHCl_3$	0.64 ± 0.015	18 ± 0.73	0.30 ± 0.014	131 ± 6.8	0.048 ± 0.0017	105
PF26:PtOEP – $CHCl_3$	0.67 ± 0.012	18 ± 0.56	0.28 ± 0.011	124 ± 5.4	0.039 ± 0.0013	97
PFO:PtOEP – Toluene	0.61 ± 0.017	15 ± 0.73	0.35 ± 0.015	112 ± 5.3	0.037 ± 0.0016	93
PF26:PtOEP – Toluene	0.66 ± 0.013	15 ± 0.55	0.30 ± 0.012	119 ± 5.1	0.036 ± 0.0013	96

Table S2. The fitting parameters of the bi-exponential functional that was applied on the TTA-UC luminescence data shown in Figure S4.

Time-gated PL spectra

Figure S5 shows that following the photoexcitation of PtOEP at 532 nm, PtOEP delayed fluorescence is detected in the ns time-scale, in the spectral region of 540 – 580 nm even when PtOEP is dispersed in the PS matrix (PS:PtOEP 6 wt%).

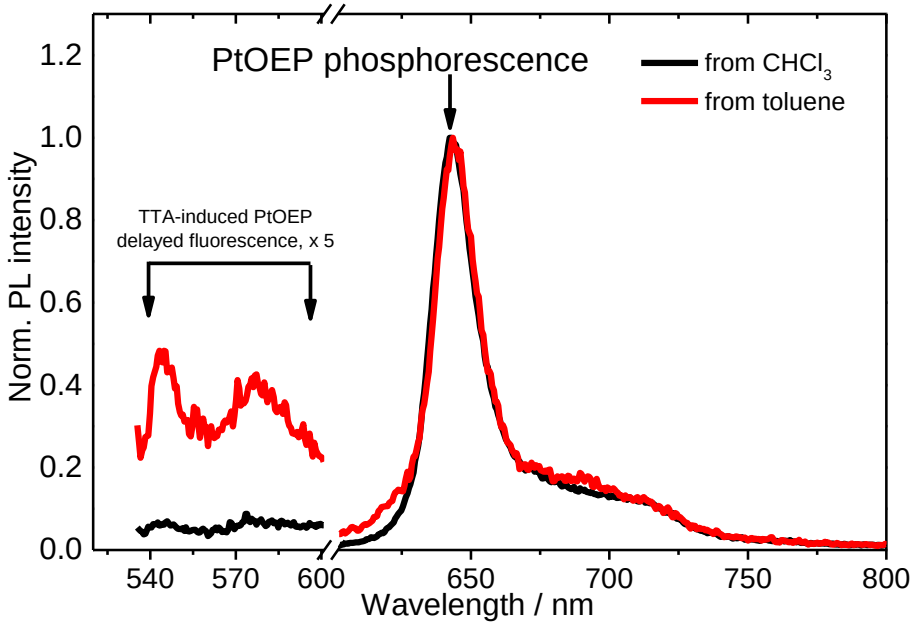

Figure S5. Normalized time-gated PL spectra of PS:PtOEP 6 wt% blend films spun from $CHCl_3$ and toluene. Optical excitation was at 530 nm and the spectra registration was with a 10 ns gate width at room temperature.

As Figure S5 presents, the intensity of PtOEP delayed fluorescence is stronger for the PS:PtOEP composite processed by toluene most likely due to the different degree of PtOEP aggregation in this system, which facilitates the TTA events within PtOEP. Atomic force microscopy (AFM) measurements performed on PS:PtOEP and PFO:PtOEP blend films spun from the two processing solvents (see Figure S7 farther below) find no differences in the surface texture of these samples, suggesting that higher resolution techniques are required to reveal the differences in PtOEP aggregation that is expected at smaller length scale.

The delayed activation of the first singlet excited state of PtOEP (S_{1_PtOEP}) is the indirect result of TTA between triplet-excited PtOEP species: following the activation of the doubly PtOEP photoexcited state D^*_{PtOEP} by TTA, internal conversion down to S_{1_PtOEP} takes place and delayed PtOEP fluorescence is produced. In the presence of a nearby activator with suitable molecular conformation such as PFO, internal conversion competes with energy transfer from D^*_{PtOEP} to PFO and the delayed PtOEP fluorescence is quenched in parallel to the activation of TTA-UC from PFO.

Figure S6 below presents a series of time-gated PL spectra of the PF26:PtOEP 6 wt% film prepared by toluene, registered with a delay-step of 10 ns, and a gate window of 10 ns. The data inform that the initially distorted PtOEP phosphorescence signal is restored after about 50 ns, thereby providing an upper limit in the time where TTA events in the PtOEP phase result in the generation of PtOEP delayed fluorescence.

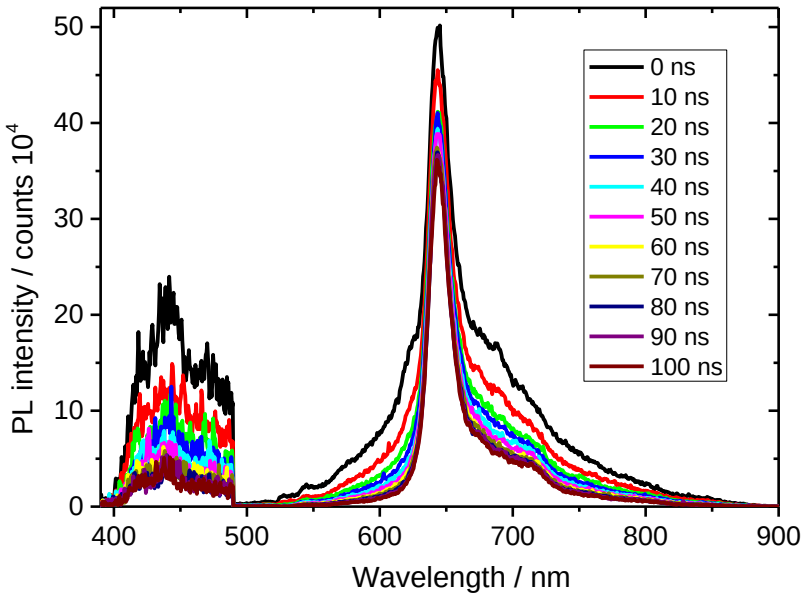

Figure S6. Room temperature, time-gated PL spectra of a PF26:PtOEP 6 wt% blend spun from toluene after photoexcitation at 532 nm. For clarity, the PL intensity of the 360 – 490 nm spectral region is multiplied by a factor of 40.

Atomic force microscopy imaging

We performed a series of AFM imaging measurements for PS:PtOEP 6 wt% and PFO:PtOEP 6 wt% films spun from $CHCl_3$ and toluene. The acquired AFM images are displayed in Figure S7 below, and the root-mean-square surface roughness (r_{rms}) of these films is reported in Table S3.

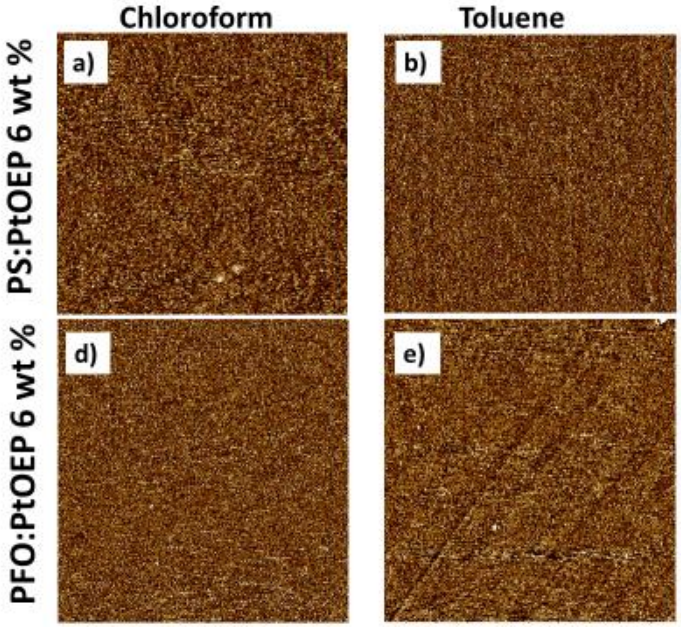

Figure S7. Tapping mode AFM phase images as obtained for the PS:PtOEP and PFO:PtOEP films spun from $CHCl_3$ and toluene based on 10 × 10 μm scans.

System	R_{rms} (nm)
PS:PtOEP 6 wt% – $CHCl_3$	0.500
PFO:PtOEP 6 wt% – $CHCl_3$	0.64
PS:PtOEP 6 wt% – Toluene	0.434
PFO:PtOEP 6 wt% – Toluene	0.760

Table S3. The r_{rms} values of the PS:PtOEP and PFO:PtOEP films as obtained from height AFM images corresponding to the data shown in Figure S7.